Supporting Information for:

A Robust Liposomal Platform for Direct Colorimetric Detection of Sphingomyelinase Enzyme and Inhibitors

Margaret N. Holme,[1,2,3,4†] Subinoy Rana,[1,2,3,5†] Hanna M. G. Barriga,[4] Ulrike Kauscher,[1,2,3] Nicholas J. Brooks,[6] Molly M. Stevens[1,2,3,4*]

[1]Department of Materials, Imperial College London, London, SW7 2AZ, UK

[2]Department of Bioengineering and [3]Institute of Biomedical Engineering, Imperial College London, London, SW7 2AZ, UK

[4]Department of Medical Biochemistry and Biophysics, Karolinska Institutet, SE-171 77 Stockholm, Sweden

[5]School of Engineering, Newcastle University, Newcastle upon Tyne, NE1 7RU, UK

[6]Department of Chemistry, Imperial College London, London, SW7 2AZ, UK

† These authors contributed equally to the work

Correspondence to:

*Email: m.stevens@imperial.ac.uk

Spectroscopic data analysis

It can be observed that the plasmon peak shifts as a function of cysteine concentration (as well as SMase concentrations). In such a case of spectral shape change, calculating the change in the ratio A/D (aggregated/dispersed area) for the area under the plasmon resonance peak provides a highly sensitive and accurate method to quantify change in spectral shape.[1,2] We calculated the A/D ratios for different cysteine concentrations, where region D spans from 480 to 545 nm and region A spans from 550 to 750 nm (Figure S1).

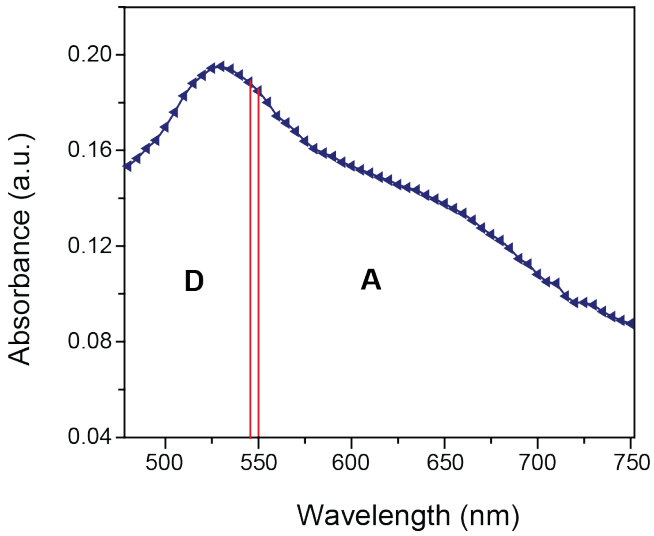

Figure S1: Plot of UV-vis spectrum showing the areas of the curve for which the integrals were computed for all samples. The spectrum corresponds to 0.6 μM cysteine added to AuNPs after 15 min incubation. Region D (Dispersion) spanning from 480 to 545 nm was chosen as representative for the single-NP plasmon resonance region while region A (Aggregation) spanning from 550 to 750 nm was chosen for the aggregated NP plasmon resonance region.

Comparison between the ratio A/D, peaks at 640 nm/525 nm, and 670 nm/525 nm showed a small difference between the methods of data treatment (Figure S2). However, the ratio A/D provided the most discernible changes among the lower concentrations. The peak ratio of 640 nm/525 nm captured the lower concentrations similar to that of A/D ratio. Therefore, for simplicity, we used changes in the ratio between absorbance at 640 nm and 525 nm, to accurately capture changes in absorbance even at lower cysteine concentrations.

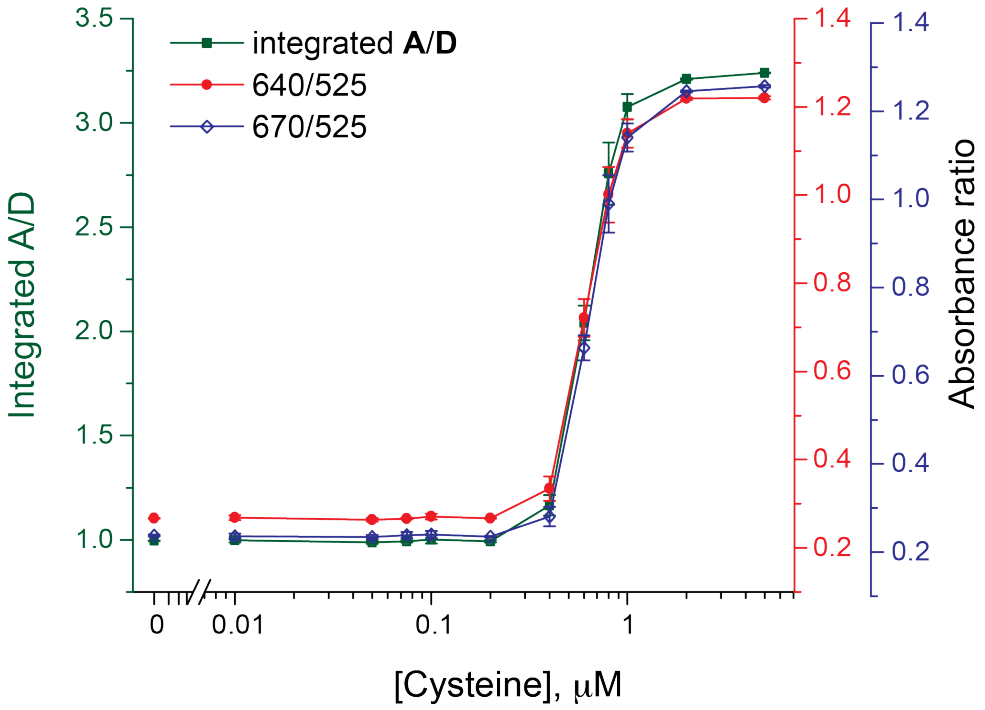

Figure S2. Comparison between the different ways of calculating the spectroscopic change with increasing cysteine concentrations.

Cysteine-mediated AuNP aggregation

The ratio of 640 nm and 525 nm corresponding to **Figure 2** is plotted below:

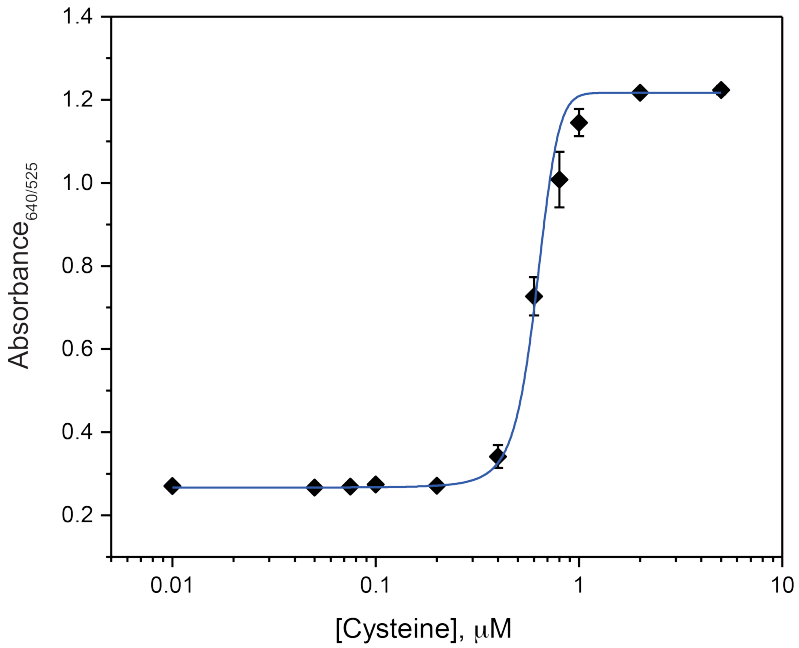

Figure S3. Effect of cysteine concentration on ratio of absorbance at 640 and 525 nm. Absorbance spectra were recorded 15 min post cysteine addition to AuNPs. The responses are the average of three independent measurements and the error bars represent the standard deviation.

Stability of liposomes over time

Liposomes loaded with 100 mM cysteine were prepared with BSM:Chol 40:60 mol% as detailed in the Materials and Methods section. Vesicles were then diluted in DPBS or DPBS with 1 mM $CaCl_2$ and 1 mM $MgSO_4$ (PMC) to a final particle concentration of 8.5 x 10^{10} particles/mL, as determined by Nanoparticle Tracking Analysis (NTA) measurements. The diluted vesicles were incubated for 1 h at r.t. then 60 µL of AuNPs were mixed with: 140 µL DPBS-diluted vesicles, 140 µL PMC-diluted vesicles, 140 µL PMC-diluted vesicles containing 4 µL Triton X-100 (1% w/v) or 140 µL DPBS only. Absorbance at 525 and 640 nm was read 15 min after addition of AuNPs, and each measurement was repeated in triplicate. We found that even after 34 days, the amount of cysteine leaked from vesicles at the vesicle concentration of 8.5 x 10^{10} particles/mL was not detectable *via* the AuNP aggregation assay.

Effect of SMase co-factors Mg^{2+} and Ca^{2+} on assay sensitivity

In order to determine the effect of Mg^{2+} and Ca^{2+} cations on SMase activity within the scope of this assay, liposomes (final concentration 8.5 x 10^{10} particles/mL) were incubated with SMase at varying final concentrations in a total volume of 140 µL. A matrix of $MgSO_4$ and $CaCl_2$ concentrations in the reaction buffer were screened, including 1, 5 and 10 mM $MgSO_4$ and 0.1, 0.5 and 1 mM $CaCl_2$. After 30 min incubation time, 60 µL of AuNPs were added. The absorbance spectrum of each well was measured from 450-750 nm, beginning at 12 min post-addition of AuNPs. Calcium is required for good activity of SMase, however we observed that the difference in SMase activity in the 0.1-1 mM calcium range investigated was negligible. In the case of magnesium, increasing concentration led to very slight increase in sensitivity. However, at 5 and 10 mM magnesium concentrations, even wells containing no SMase led to purple colored solutions. This is undesirable for naked eye detection, which requires a colorimetric response, where the difference between red, purple and blue is much easier to differentiate by eye than the difference between a range of purple hues and blue. Therefore, a concentration of 1 mM $MgSO_4$ was selected since this led to a red color in the absence of SMase, due to baseline absorbance ratios of less than 0.3.

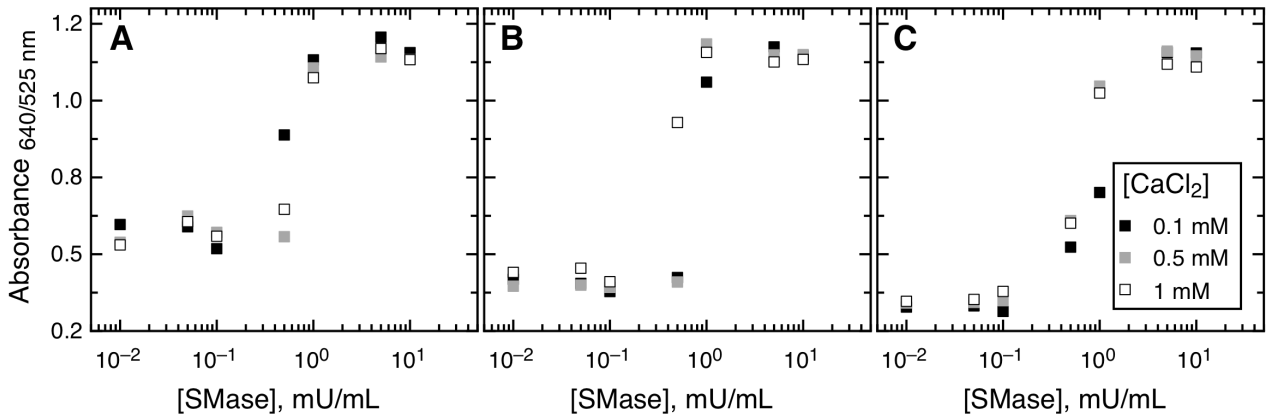

Figure S4: Characterization of Mg^{2+} and Ca^{2+} concentrations required for optimal enzyme activity. A, 10 mM $MgSO_4$; B, 5 mM $MgSO_4$; C, 1 mM $MgSO_4$. Each point is a single measurement.

Effect of liposome concentration on background absorbance ratio

Liposomes loaded with 100 mM cysteine were prepared with BSM:Chol 40:60 mol% as detailed in the Materials and Methods section. The particle concentration of the sample after size exclusion chromatography was determined by NTA as 1.9 x 10^{12} particles/mL. Vesicles were then diluted in DPBS with 1 mM $CaCl_2$ and 1 mM $MgSO_4$ (PMC) to final particle concentrations of 2.7 x 10^{11}, 1.7 x 10^{11}, 8.6 x 10^{10}, 4.3 x 10^{10} and 1.4 x 10^{10} particles/mL. 140 µL of the diluted vesicles were incubated for 1 h at r.t. then 60 µL of AuNPs were added. As a negative control, 60 µL of AuNPs were also added to 140 µL of PMC treated in the same manner. Absorbance at 525 and 640 nm was read 15 min after addition of AuNPs, and each measurement was repeated in triplicate. We observed that 8.6 x 10^{10} particles/mL was the highest measured concentration where, in the absence of SMase, the amount of cysteine that leaked from the vesicles within the assay timeframe was not higher than the control (see Figure S5). We therefore concluded that this concentration was optimal for maximum encapsulated cysteine whilst maintaining background stability and all further experiments were conducted with a final particle concentration rounded to 8.5 x 10^{10} particles/mL, determined for each vesicle batch by NTA.

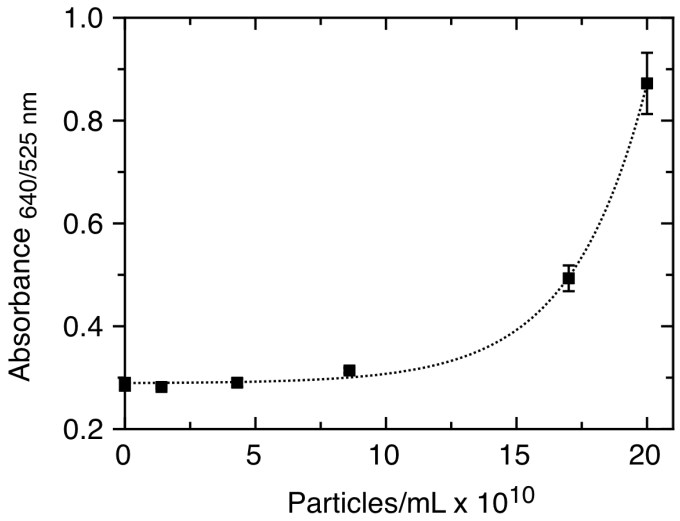

Figure S5. Effect of liposome concentration on background ratio of absorbance at 640 and 525 nm. Absorbance spectra were recorded 15 min post cysteine addition to AuNPs. The responses are the average of three independent measurements and the error bars represent the standard deviation.

SAXS and WAXS studies

The diffraction patterns for all the compositions are shown below.

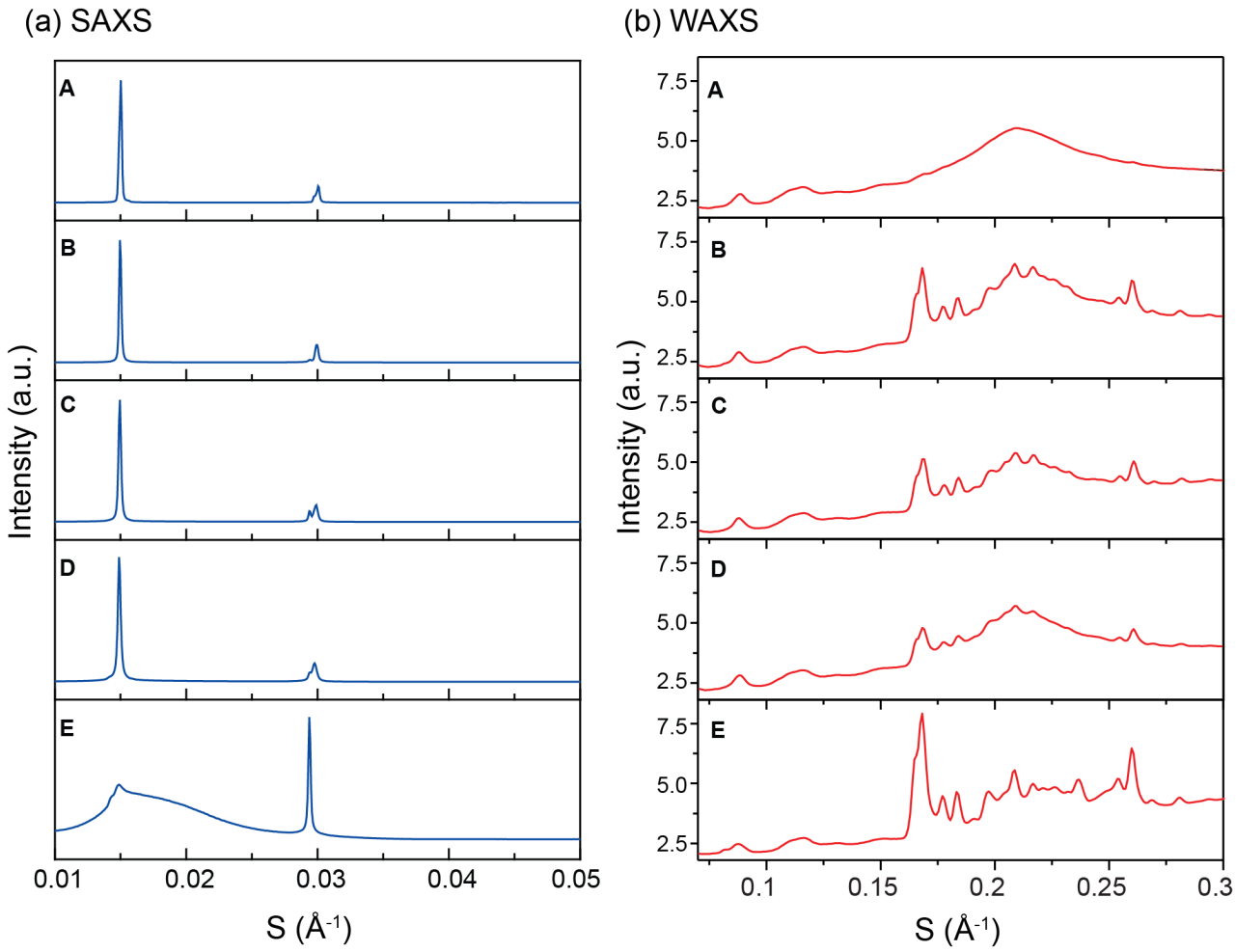

Figure S6: SAXS and WAXS characterization of BSM:BC:Chol mixtures. Bulk (a) SAXS and (b) WAXS measurements of lipid packing of mixtures containing the following mol% of BSM:BC:Chol: **A**, 40:0:60; **B**, 36:4:60; **C**, 32:8:60; **D**, 28:12:60 and **E**, 20:20:60.

Measurement of vesicle size and concentration by NTA

The liposome fraction collected after separation of unencapsulated cysteine by size exclusion chromatography was diluted 1000x in DPBS and measured in triplicate using a NanoSight NS300 at camera intensity 13 for 60 sec. Data was analysed within the NanoSight software analysis program with screen gain 1, and detection threshold 5. The average of three measurements was used to determine mean particle diameter and vesicle concentration.

Transmission Electron Microscopy

TEM of AuNPs: Carbon film on Cu-200 mesh EM Grids (Electron Microscopy Supplies) were loaded with 4 µL of sample on the carbon side and incubated for 5 min before blotting with filter paper and drying at r.t. overnight. Images were acquired using a JEOL 2100 Plus Transmission Electron Microscope and Gatan Orius SC 1000 camera at 30k and 50k magnification.

CryoTEM of liposome formulations: Holey Carbon on Cu-200 mesh EM Grids (Electron Microscopy Supplies) were glow-discharged (15 sec with O_2/H_2 1:1 on a Gatan SOLARIS plasma cleaner). Using a Leica EM GP plunge freezer, 4 µL samples were loaded onto the carbon side of the plasma-treated grids, which were incubated for 30 sec at 90% humidity and blotted twice for 1 sec using filter paper immediately prior to vitrification. After vitrification, grids were stored under liquid nitrogen until further use. Grids were mounted in a Gatan 914 cryo-holder for cryo-EM imaging on a JEOL 2100 Plus Transmission Electron Microscope using Minimum Dose System software. Images were acquired over 2 sec exposure times, using a Gatan Orius SC 1000 camera at 30k and 40k magnification and a defocus of -2.5 µm.

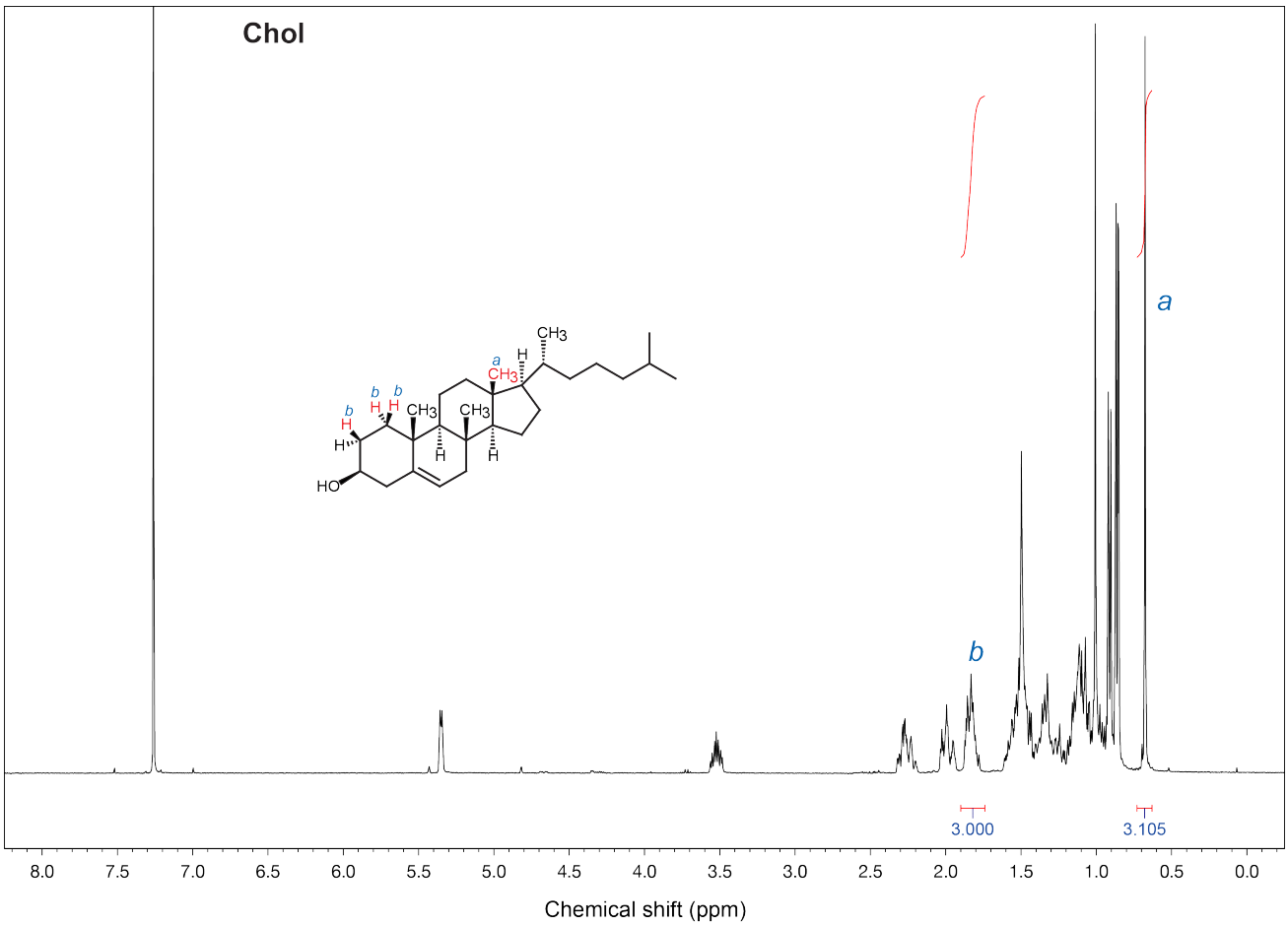

Figure S7: ^{1}H NMR spectrum of Chol in $CDCl_3$. Two non-overlapping signature peaks are assigned to the protons *a* (3H) and *b* (3H) at 1.84 and 0.68 ppm, respectively, which are unique chemical shifts for Chol.[3,4] The integrals at these peaks have been used in analysing the BSM:Chol liposome ratios.

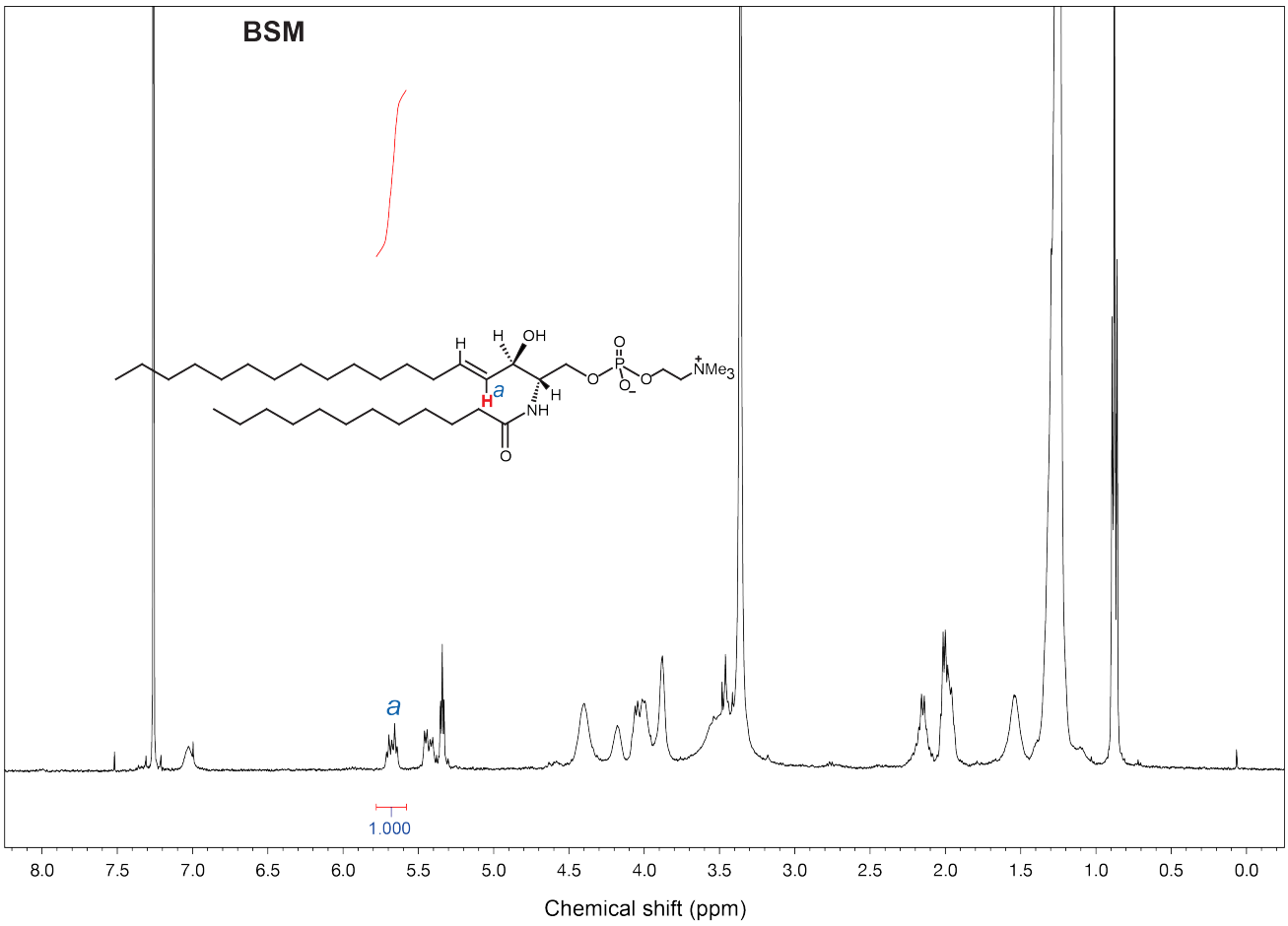

Figure S8: ^{1}H NMR spectrum of BSM in $CDCl_3$. One signature peak assigned to the proton *a* (1H) at 5.70 ppm that is unique chemical shift for BSM.[5] The integrals at this peak have been used in analysing the BSM:Chol liposome ratios.

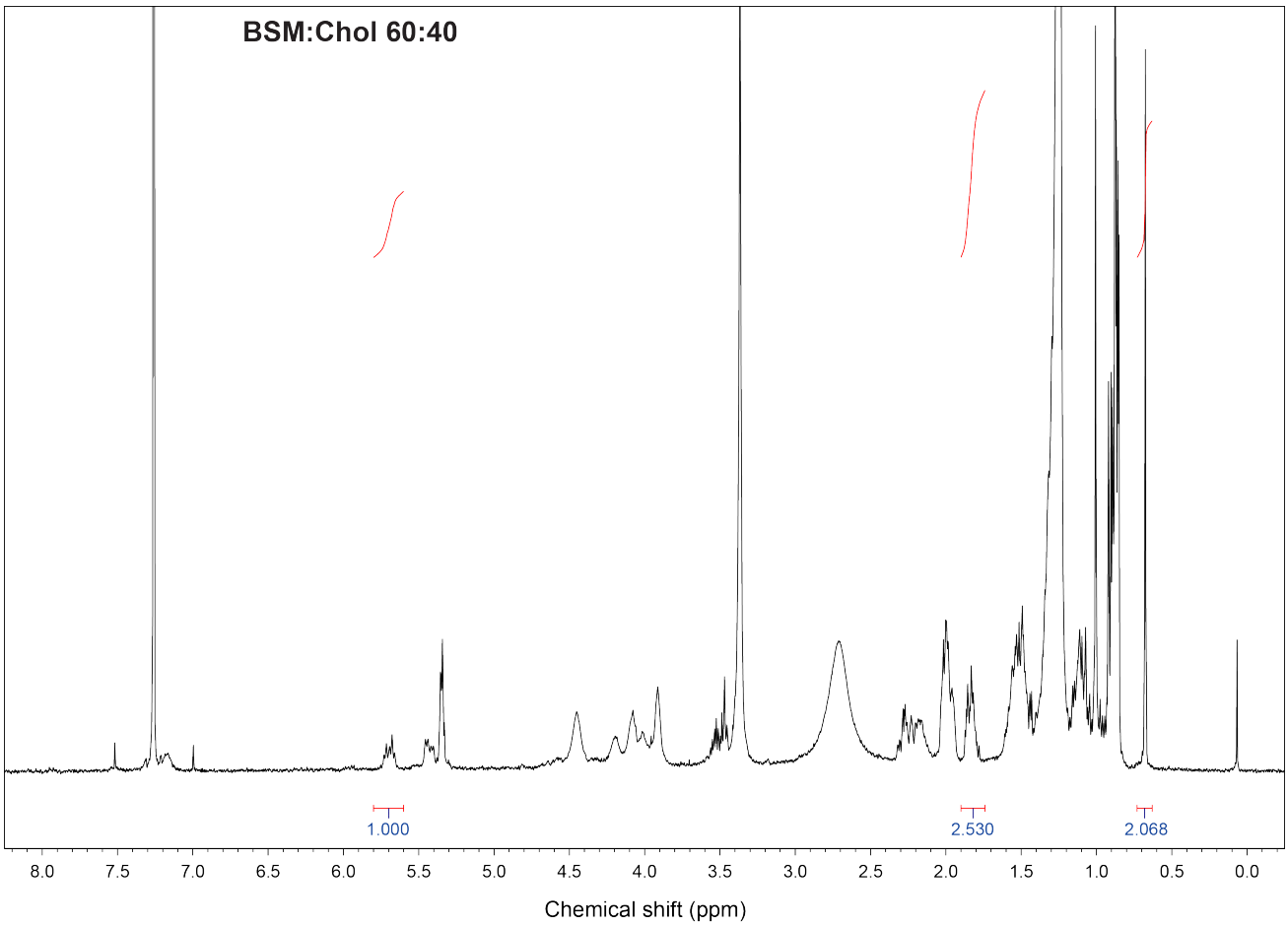

Figure S9: ^{1}H NMR spectrum in $CDCl_3$ of a lyophilized sample of BSM/Chol liposomes prepared from a BSM:Chol 60:40 mol% lipid film, hydrated in pure water and extruded 31 times over a 100 nm polycarbonate membrane.

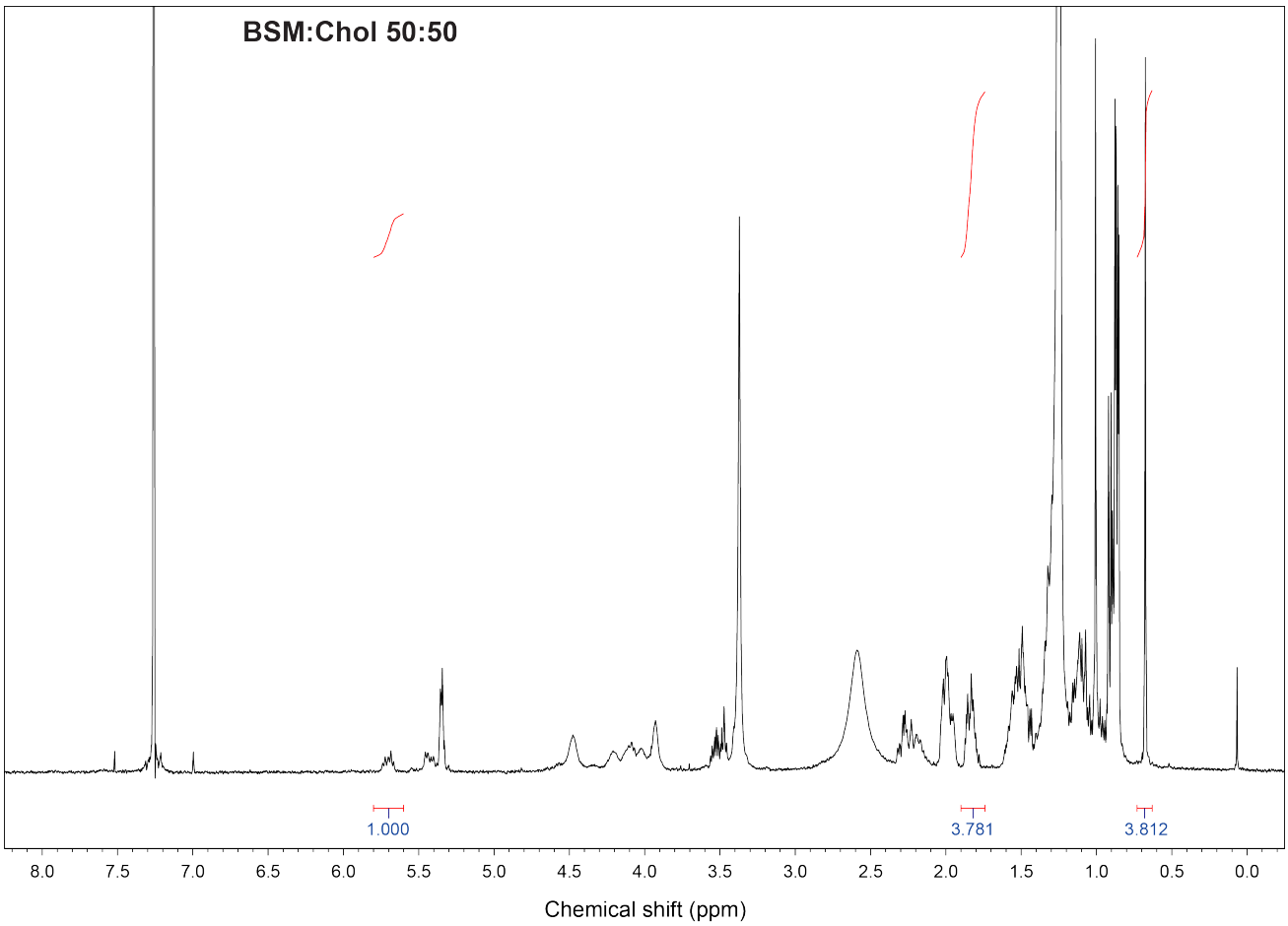

Figure S10: ^{1}H NMR spectrum in $CDCl_3$ of a lyophilized sample of BSM/Chol liposomes prepared from a BSM:Chol 50:50 mol% lipid film, hydrated in pure water and extruded 31 times over a 100 nm polycarbonate membrane.

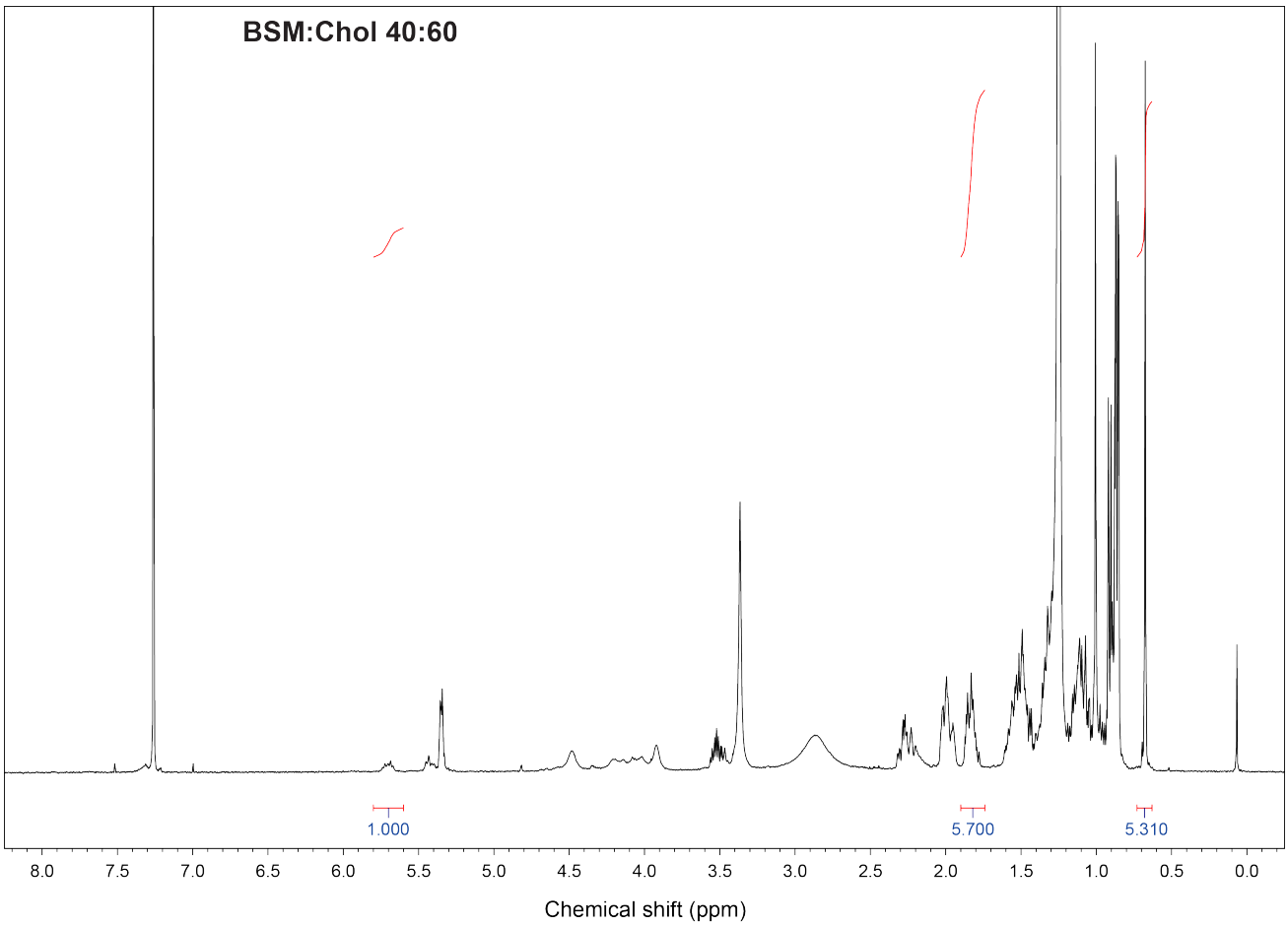

Figure S11: ^{1}H NMR spectrum in $CDCl_3$ of a lyophilized sample of BSM/Chol liposomes prepared from a BSM:Chol 40:60 mol% lipid film, hydrated in pure water and extruded 31 times over a 100 nm polycarbonate membrane.

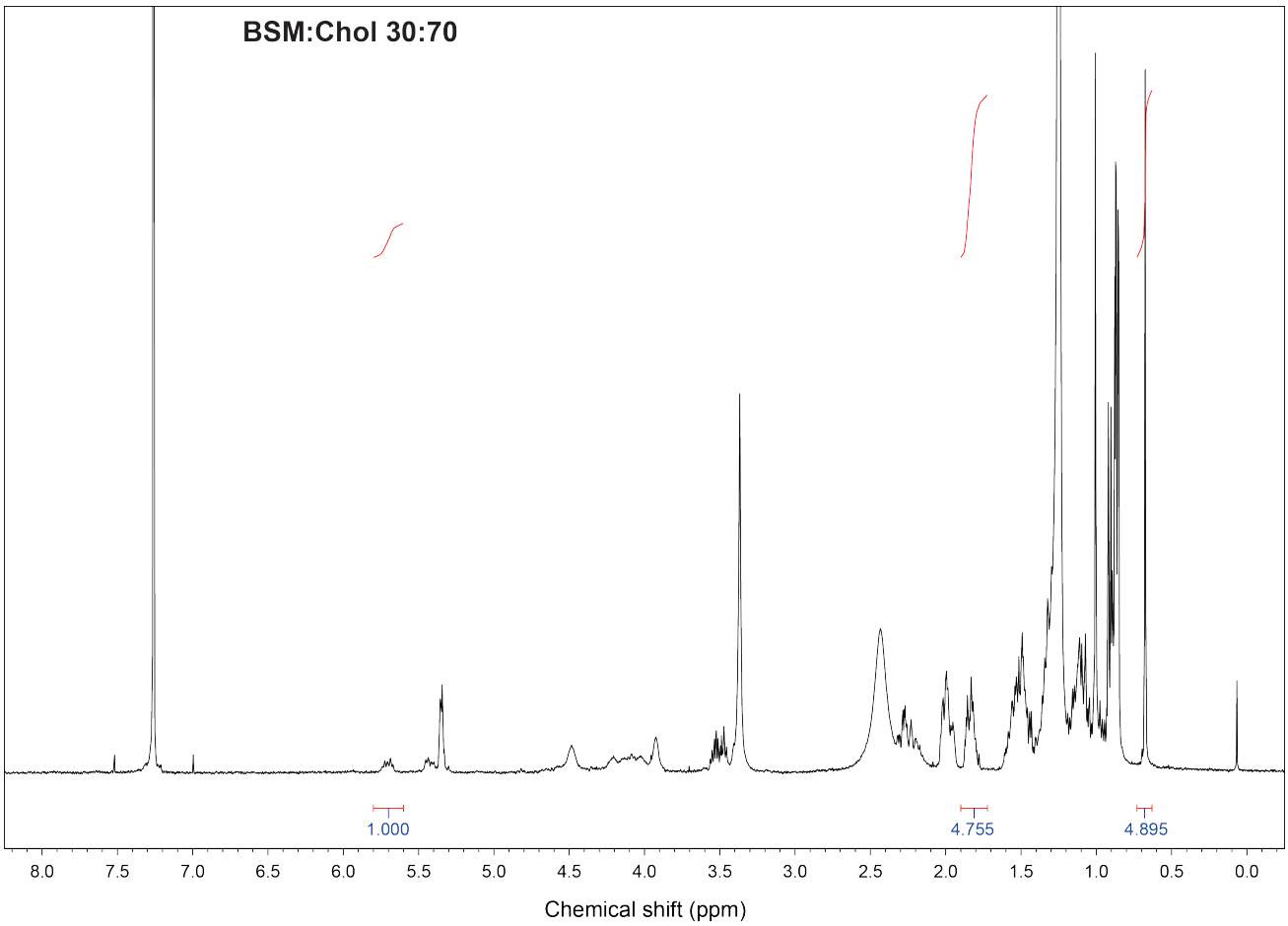

Figure S12: ^{1}H NMR spectrum in $CDCl_3$ of a lyophilized sample of BSM/Chol liposomes prepared from a BSM:Chol 30:70 mol% lipid film, hydrated in pure water and extruded 31 times over a 100 nm polycarbonate membrane.

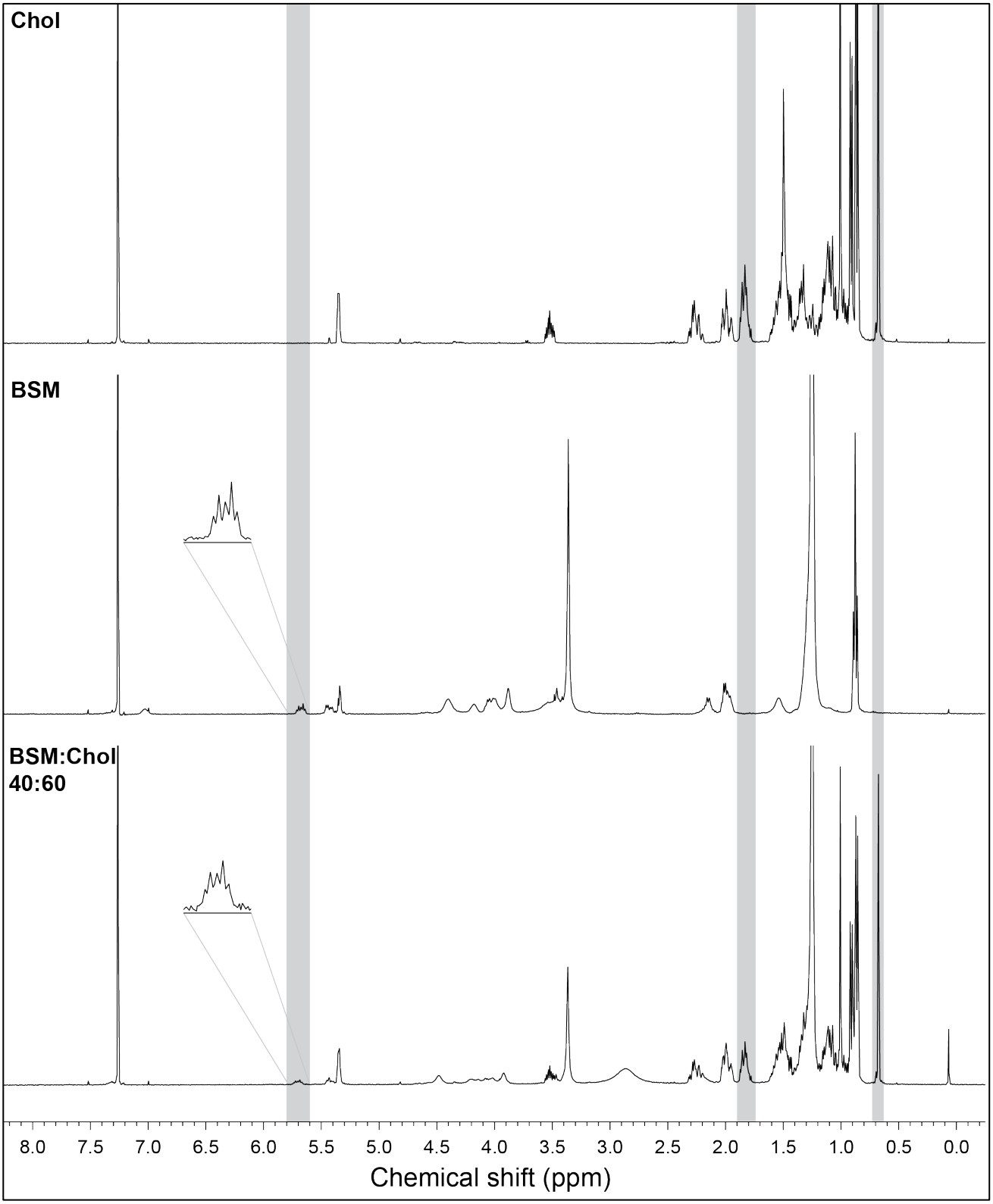

Figure S13**:** Overlaid spectra from Figures S7, S8 and S11 showing integrated regions used in analysis of BSM:Chol liposome ratios.

References

1. Laromaine, A.; Koh, L.; Murugesan, M.; Ulijn, R. V.; Stevens, M. M., Protease-Triggered Dispersion of Nanoparticle Assemblies. *J. Am. Chem. Soc.* **2007,** *129*, 4156-57.
2. Chowdhury, M. H.; Julian, A. M.; Coates, C. J.; Coté, G. L., Detection of Differences in Oligonucleotide-Influenced Aggregation of Colloidal Gold Nanoparticles Using Absorption Spectroscopy. *J. Biomed. Opt.* **2004**, *9*, 1347-57.
3. Iida, T.; Tamura, T.; Matsumoto, T., Proton Nuclear Magnetic Resonance Identification and Discrimination of Side Chain Isomers of Phytosterols Using A Lanthanide Shift Reagent. *J. Lipid Res.* **1980,** *21*, 326-38.
4. Sawan, S. P.; James, T. L.; Gruenke, L. D.; Craig, J. C., Proton NMR Assignments for Cholesterol. Use of Deuterium NMR as an Assignment Aid. *J. Magn. Reson.* **1979,** *35*, 409-13.
5. Adosraku, R. K.; Choi, G. T. Y.; Constantinou-Kokotos, V.; Anderson, M. M.; Gibbons, W. A., NMR Lipid Profiles of Cells, Tissues, and Body Fluids: Proton NMR Analysis of Human Erythrocyte Lipids. *J. Lipid Res.* **1994,** *35*, 1925-31.